Ceramide Mediates Vascular Dysfunction in Diet-Induced Obesity by PP2A-Mediated Dephosphorylation of the eNOS-Akt Complex

Quan-Jiang Zhang,[1,2,3] William L. Holland,[4] Lloyd Wilson,[1] Jason M. Tanner,[1] Devin Kearns,[1] Judd M. Cahoon,[1] Dix Pettey,[1] Jason Losee,[1] Bradlee Duncan,[1] Derrick Gale,[1] Christopher A. Kowalski,[1] Nicholas Deeter,[1] Alexandrea Nichols,[1] Michole Deesing,[1] Colton Arrant,[1] Ting Ruan,[2] Christoph Boehme,[5] Dane R. McCamey,[5] Janvida Rou,[5] Kapil Ambal,[5] Krishna K. Narra,[2] Scott A. Summers,[6] E. Dale Abel,[2,3] and J. David Symons[1,2]

Vascular dysfunction that accompanies obesity and insulin resistance may be mediated by lipid metabolites. We sought to determine if vascular ceramide leads to arterial dysfunction and to elucidate the underlying mechanisms. Pharmacological inhibition of de novo ceramide synthesis, using the Ser palmitoyl transferase inhibitor myriocin, and heterozygous deletion of dihydroceramide desaturase prevented vascular dysfunction and hypertension in mice after high-fat feeding. These findings were recapitulated in isolated arteries in vitro, confirming that ceramide impairs endothelium-dependent vasorelaxation in a tissue-autonomous manner. Studies in endothelial cells reveal that de novo ceramide biosynthesis induced protein phosphatase 2A (PP2A) association directly with the endothelial nitric oxide synthase (eNOS)/Akt/Hsp90 complex that was concurrent with decreased basal and agonist-stimulated eNOS phosphorylation. PP2A attenuates eNOS phosphorylation by preventing phosphorylation of the pool of Akt that colocalizes with eNOS and by dephosphorylating eNOS. Ceramide decreased the association between PP2A and the predominantly cytosolic inhibitor 2 of PP2A. We conclude that ceramide mediates obesity-related vascular dysfunction by a mechanism that involves PP2A-mediated disruption of the eNOS/Akt/Hsp90 signaling complex. These results provide important insight into a pathway that represents a novel target for reversing obesity-related vascular dysfunction. ***Diabetes* 61:1848–1859, 2012**

From the [1]College of Health, University of Utah, Salt Lake City, Utah; the [2]Division of Endocrinology, Metabolism, and Diabetes, University of Utah School of Medicine, Salt Lake City, Utah; the [3]Program in Molecular Medicine, University of Utah, Salt Lake City, Utah; the [4]Touchstone Diabetes Center, University of Texas Southwestern Medical Center, Dallas, Texas; the [5]Department of Physics and Astronomy, College of Science, University of Utah, Salt Lake City, Utah; and the [6]Program in Cardiovascular and Metabolic Diseases, Duke-NUS Graduate Medical School, Singapore, and the Stedman Center for Nutrition and Metabolism Research, Duke University Medical Center, Durham, North Carolina.

Corresponding authors: E. Dale Abel, dale.abel@hmbg.utah.edu, and J. David Symons, j.david.symons@hsc.utah.edu.

Received 4 October 2011 and accepted 29 February 2012.

DOI: 10.2337/db11-1399

This article contains Supplementary Data online at http://diabetes.diabetesjournals.org/lookup/suppl/doi:10.2337/db11-1399/-/DC1.

Q.-J.Z. and W.L.H. contributed equally to the study.

© 2012 by the American Diabetes Association. Readers may use this article as long as the work is properly cited, the use is educational and not for profit, and the work is not altered. See http://creativecommons.org/licenses/by-nc-nd/3.0/ for details.

The prevalence of obesity in the U.S. exceeds 30% and contributes to type 2 diabetes and insulin resistance (1). Cardiovascular complications are the leading cause of death in patients with diabetes. Therefore, elucidating mechanisms responsible for vascular dysfunction in individuals with diet-induced obesity and diabetes is of high priority.

Obesity, type 2 diabetes, and metabolic syndrome are associated with elevated circulating concentrations of free fatty acids (FFAs) (2). Studies in cultured cells (3,4), isolated arteries (4,5), animal models (4,6), and humans (7) demonstrate that elevated FFAs impair nitric oxide (NO) production. NO is ubiquitous, and the bioavailability of this signaling molecule depends on a delicate balance between factors responsible for its synthesis and its degradation. Endothelial cell–derived NO has vasodilatory, anti-inflammatory, and antiproliferative properties (8–10). Thus, any mismatch between generation and degradation of this molecule potentially could precipitate cardiovascular complications.

When FFA accumulation exceeds adipose storage and oxidative capacity, they are ectopically deposited into tissues not suited for lipid storage (e.g., skeletal muscle, liver), leading to accumulation of bioactive lipid metabolites, which are associated with metabolic dysfunction and cardiovascular risk. One such metabolite is the sphingolipid ceramide (11,12). Obesity and lipid exposure promote sphingolipid accumulation in peripheral tissues of rodents and humans, and ceramide recently was reported to accumulate in arteries from a rat model of uncontrolled type 2 diabetes (13).

A strong rationale exists to test the hypothesis that vascular ceramide contributes to cardiovascular complications. In several cell types, ceramide disrupts signaling kinases that phosphorylate endothelial NO synthase (eNOS) at positive regulatory sites (14) and potentiates signaling kinases that phosphorylate eNOS at negative regulatory sites (11,15). Short-term incubation with synthetic ceramide impairs endothelium-dependent vasorelaxation (EDR) (16), exaggerates vasocontraction of isolated arteries (17), and reduces the bioavailability of NO in human endothelial cells (18). In rodent models of lipid oversupply, targeted inhibition of ceramide biosynthesis via pharmacological or genetic approaches attenuates metabolic disturbances (13,19–22), atherosclerotic lesion formation (13,23,24), and endothelium-dependent dysfunction (13). In the latter study, administration

of the ceramide synthesis inhibitor myriocin to fat-fed rats given streptozotocin reduced arterial ceramide content and partially reversed endothelial dysfunction in parallel with amelioration of the metabolic milieu (13). While these results suggest that endogenous ceramide synthesis might precipitate cardiovascular complications, it is difficult to discern whether improved arterial function resulted from lower vascular ceramide accrual or from improvement in the systemic environment.

We hypothesized that vascular ceramide accumulates in response to high-fat (HF) feeding and that limiting this increase would negate arterial dysfunction and hypertension in mice with diet-induced obesity. We show for the first time that vascular ceramide accrual in obese and insulin-resistant mice precipitates endothelial dysfunction and impairs eNOS phosphorylation in a tissue-autonomous manner. Inhibition of de novo ceramide biosynthesis in isolated arteries exposed to palmitate recapitulate the in vivo studies, providing further evidence that ceramide directly impairs EDR. In bovine aortic endothelial cells (BAECs), palmitate increased de novo ceramide synthesis, which reduced agonist-stimulated eNOS phosphorylation and dimer formation. These changes were not the result of impaired upstream signaling to eNOS from Akt, AMP-activated protein kinase (AMPK), or extracellular signal–related kinase (ERK) 1/2 or to superoxide anion ($O_2^{\cdot -}$)-mediated peroxynitrite formation. Rather, ceramide accumulation induced colocalization of the protein phosphatase 2A (PP2A) with eNOS, which reduced eNOS phosphorylation, prevented its association with Hsp90 and Akt, and decreased the phosphorylation of the pool of Akt that associates directly with eNOS. Ceramide might initiate PP2A colocalization with eNOS by disrupting the interaction between inhibitor 2 of PP2A (I2PP2A) and PP2A. These results define an important role for endogenous ceramide accumulation in the pathogenesis of vascular dysfunction and significantly extend previous knowledge (14) regarding how ceramide modulates endothelial cell function.

RESEARCH DESIGN AND METHODS

Animal studies. Experiments were performed using *1*) 10-week-old C57Bl/6 mice that consumed standard (CON) chow (Research Diets Inc., New Brunswick, NJ) containing (kilocalories) 10% fat, 70% carbohydrate, and 20% protein (D12450B) or HF chow containing (kilocalories) 45% fat, 35% carbohydrate, and 20% protein (D12451) for 12–13 weeks; *2*) 12-week-old wild-type ($des1^{+/+}$) and $des1^{+/-}$ mice on the C57Bl/6J background; and *3*) 10-week-old $des1^{+/+}$and $des1^{+/-}$ mice that consumed CON or HF chow for 12–13 weeks. Metabolic and cardiovascular phenotyping was performed during the final 2–3 weeks of the feeding studies (4,19). Terminal experiments were performed after mice were anesthetized (2–5% isoflurane) after an overnight fast. The entire aorta and both iliac and femoral arteries were isolated and used for immunoblotting and ceramide analyses and to assess vascular function. All protocols were approved by the institutional animal care and use committee.

Immunoblotting. Arteries were processed for immunoprecipitation and immunoblotting as described (4,25,26).

Ceramide. Aortic ceramide content was assessed using a modified diacylglycerol kinase assay (19,27) or by high-performance liquid chromatography with tandem mass spectrometry in studies of $des1^{+/-}$ and $des1^{+/+}$ mice (28).

Vascular function. Vascular reactivity was assessed in femoral arteries (~150 μm internal diameter) using isometric tension techniques (4,26).

Cell culture studies. BAECs were grown in Dulbecco's modified Eagle's medium supplemented with 10% FBS, human epidermal growth factor, and antibiotics (10,000 units/mL penicillin and 10 μg/mL streptomycin) in a humidified atmosphere (5% CO_2/95% O_2) at 37°C. When cells were 70–80% confluent, they were passaged and transferred to appropriately sized culture plates. Palmitate was coupled to fatty acid–free BSA in the ratio of 2 mol/L palmitate to 1 mol/L BSA (4,19). For most experiments, BAECs were treated for 3 h with *1*) 1% BSA plus 0.2% methanol (vehicle), *2*) 1% BSA plus 10 μmol/L myriocin, *3*) vehicle plus 500 μmol/L palmitate, or *4*) myriocin plus palmitate. For experiments assessing protein phosphorylation, 100 nmol/L insulin or 10 ng/mL vascular endothelial cell growth factor (VEGF), or their vehicle (PBS), was added for the last 10 min of the 180-min treatment period. Tiron (1 mmol/L) or 4 nmol/L okadaic acid (OA) was used in some experiments to inhibit $O_2^{\cdot -}$ or PP2A, respectively. After 3 h, cells were treated as appropriate to assess ceramide biosynthesis (19,27) and to perform the following experiments.

Nitrate plus nitrite production and NOS activity. Nitrate plus nitrite (NO_x) production was assessed using amperometric probes and NOS activity was measured using a commercially available kit (4,25).

Reactive oxygen species and $O_2^{\cdot -}$ production. Reactive oxygen species (ROS) were assessed using 2′,7′ dichlorodihydrofluorescein diacetate (H_2DCFDA-AM), and $O_2^{\cdot -}$ production was measured using electron spin/paramagnetic resonance spectroscopy (ESR) and dihydroethidium staining (4).

Nitrotyrosine formation. Nitrotyrosine was assessed via enzyme-linked immunosorbent assay, Western blot, and immunostaining.

Superoxide dismutase activity. Total superoxide dismutase (SOD) and SOD2 enzyme activity was measured using a commercially available kit.

Short interference RNA generation and transfection. PP2A knockdown was conducted using short interference (si)RNA as described (14).

Statistics. Data are presented as mean ± SEM. Significance was accepted at $P < 0.05$. Comparison of one time point among groups was made using a one-way ANOVA. Comparison of multiple time points among groups was made using a one-way or two-way repeated-measures ANOVA. Tukey post hoc tests were performed when significant main effects were obtained.

RESULTS

Inhibiting de novo ceramide accumulation improves systemic metabolic homeostasis in C57Bl/6 mice with diet-induced obesity. After 3 months of HF feeding starting at 10 weeks of age, vascular and liver ceramide content were increased by 73 and 142%, respectively, relative to animals on a CON diet (Fig. 1*A* and *B*). Myriocin inhibits Ser palmitoyl transferase 1, the rate-limiting enzyme responsible for de novo ceramide synthesis. Concurrent treatment with myriocin prevented diet-induced ceramide accumulation. HF animals demonstrated increased body and fat mass, decreased lean mass, impaired glucose and insulin tolerance, and elevated circulating triglyceride, leptin, and catecholamine concentrations (Fig. 1*C*–*I* and Supplementary Fig. 1*A*–*D*), which were attenuated by myriocin, confirming recent reports (13,19,20).

Inhibiting de novo ceramide accumulation normalizes endothelial dysfunction and systemic hypertension in C57Bl/6 mice with diet-induced obesity. Diurnal blood pressure was elevated in vehicle-treated mice that consumed HF diets (Fig. 2*A*–*C* and Supplementary Fig. 2*A*–*D*). EDR was impaired in vehicle-treated HF mice, while endothelium-independent vasorelaxation (EIR) was similar across all treatments (Fig. 2*D*–*E*). Developed tension in response to potassium chloride or phenylephrine was greater in vessels from vehicle-treated HF mice versus all other groups (Fig. 2*F* and *G*), which is consistent with impaired NO production. Obesity-related hypertension and vascular dysfunction were prevented by myriocin treatment.

Consistent with our previous investigation (4), basal eNOS phosphorylation at Ser1177 was reduced in arteries from vehicle-treated HF mice versus all groups, in the absence of any defects in Akt, AMPK, or ERK 1/2 phosphorylation (not shown), and was prevented by myriocin treatment (Fig. 2*H*). Thus, endogenous vascular ceramide accumulation likely mediates arterial hypertension and vascular dysfunction by reducing NO production.

Arterial dysfunction is prevented in fat-fed mice with targeted disruption of dihydroceramide desaturase. To this point, our data and those from others (13) cannot distinguish if the beneficial effect of myriocin was secondary to reduced vascular ceramide accrual or from improvement

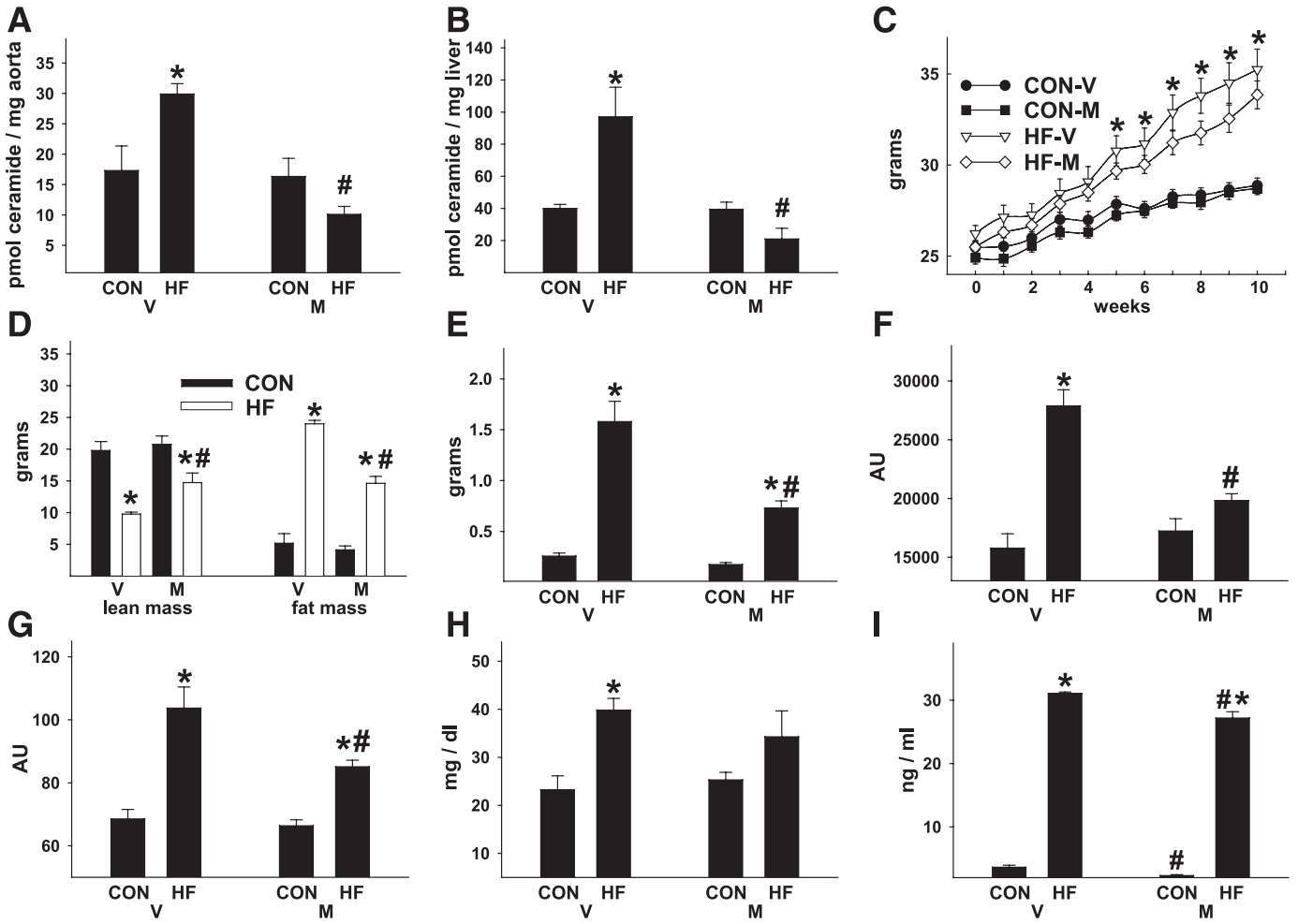

FIG. 1. Inhibiting de novo ceramide accumulation improves the systemic metabolic environment of C57Bl/6 mice with diet-induced obesity. C57Bl/6 mice that consumed CON or HF chow for 3 months were treated concurrently with vehicle (V) or myriocin (M). Vascular (aorta) (*A*) and liver (*B*) ceramide content, body mass (*C*), body composition (*D*), gonadal fat pad mass (*E*), area under the curve during a glucose tolerance test (GTT) (*F*) and insulin tolerance test (*G*). Fasting (6 h) serum triglycerides (*H*) and serum leptin (*I*) concentrations. Fasting (6 h) blood glucose (mg/dL) before the GTT in panel *F* was higher in HF-V (122 ± 8) vs. CON-V (95 ± 7) mice but was similar between HF-M (102 ± 5) and CON-M (96 ± 5) animals. *$P < 0.05$ CON vs. HF, #$P < 0.05$ M vs. V. Results represent mean ± SEM from 10 CON-V, 13 HF-V, 7 CON-M, and 13 HF-M mice. AU, arbitrary unit.

in the metabolic milieu. We therefore examined male mice with heterozygous deletion of one allele of dihydroceramide desaturase 1 (des1$^{+/-}$) and wild-type littermates (des1$^{+/+}$) (19) after CON or HF feeding. Des1 converts metabolically inactive dihydroceramide into active ceramide. Homozygous null (des1$^{-/-}$) mice fail to thrive, but des1$^{+/-}$ animals have a normal life span (19). Arterial ceramide was increased by HF feeding in des1$^{+/+}$ but not des1$^{+/-}$ mice (Fig. 3*A*). HF animals developed increased body and fat mass, decreased lean mass, and impaired glucose tolerance, which were more severely altered in des1$^{+/-}$ versus des1$^{+/+}$ mice (Fig. 3*B* and *C* and Supplementary Fig. 3*A*–*C*). Thus, fat-fed des1$^{+/-}$ mice develop metabolic disturbances but do not accumulate ceramide in the vasculature. EDR was impaired, and nonreceptor (NR)- and receptor-mediated (not shown) vasocontraction was exaggerated in arteries from HF des1$^{+/+}$ but not des1$^{+/-}$ mice (Fig. 3*D*–*G*). EIR was similar among groups (Fig. 3*H*). Fat feeding reduced basal phosphorylated (p)-eNOS Ser1177 to a greater extent in arteries from des1$^{+/+}$ versus des1$^{+/-}$ mice (Fig. 3*I*). Consistent with our earlier study (4), and in fat-fed C57Bl/6 mice shown earlier, HF feeding did not alter Akt phosphorylation in the vasculature of either des1$^{+/+}$ or des1$^{+/-}$ mice (not shown). Thus, inhibiting ceramide synthesis in vivo prevents vascular dysfunction despite an abnormal metabolic milieu.

Inhibition of ceramide synthesis prevents palmitate-induced vascular dysfunction in isolated vessels. Isolated arteries were incubated for 3 h with palmitate prebound with albumin to a final concentration of 500 μmol/L palmitate. Palmitate is a prevalent circulating saturated FFA that is the precursor for ceramide biosynthesis (5,29), and 500 μmol/L mimics circulating pathophysiological conditions (5,29). Three hours of palmitate incubation increased ceramide content in aorta from C57Bl/6 mice by 20%, which was negated by myriocin (Fig. 4*A*). EDR of arteries from the same mice was impaired by palmitate and reversed by myriocin (Fig. 4*B*). There was no decrease in sodium nitroprusside–mediated vasorelaxation, indicating an endothelium-specific defect (Fig. 4*C*). p-eNOS Ser1177 to total eNOS was reduced in palmitate-exposed aorta, and this response was prevented by myriocin (Fig. 4*G*).

Similar experiments were performed in vessels isolated from des1$^{+/+}$ and des1$^{+/-}$ mice. On CON chow, body composition, glucose tolerance, serum insulin, and triglyceride

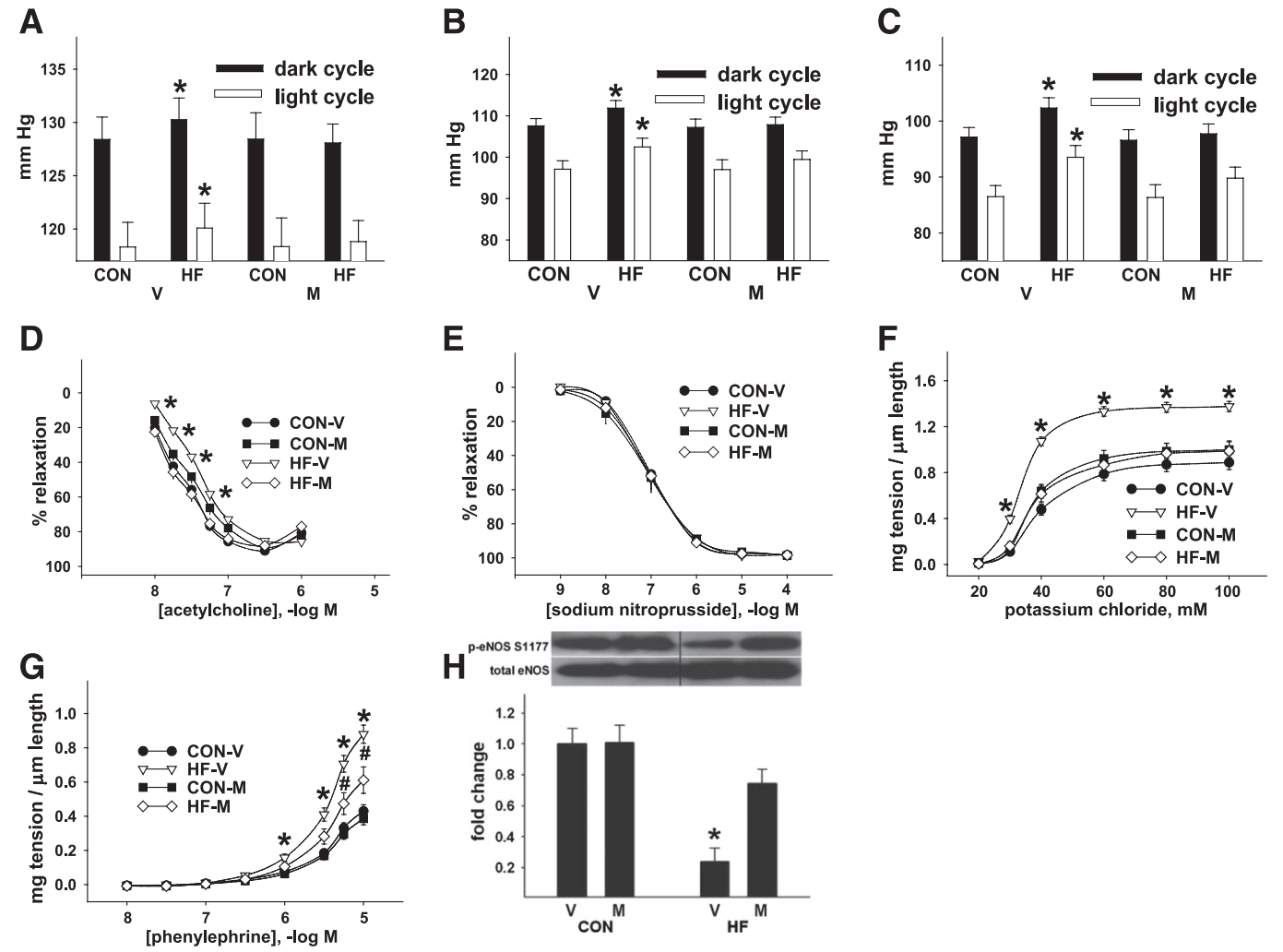

FIG. 2. Inhibiting de novo ceramide accumulation in vivo normalizes endothelial dysfunction and hypertension in C57Bl/6 mice with diet-induced obesity. Systolic (*A*), mean (*B*), and diastolic (*C*) arterial blood pressure during light and dark cycles. Data are averaged from 4- × 24-h periods for 10 CON-V, 10 HF-V, 9 CON-M, and 9 HF-M mice. *D*: EDR. *E*: EIR. *F*: NR-mediated vasocontraction. *G*: Receptor (R)-mediated vasocontraction. Data are from two femoral artery segments from 18 CON-V, 23 HF-V, 15 CON-M, and 17 HF-M mice. *A–H*: *$P < 0.05$ HF-V vs. all. *G*: #$P < 0.05$ HF-M vs. all. Results represent mean ± SEM. *H*: Representative immunoblot and densitometry of the ratio of p-eNOS at serine (S) 1177 to total eNOS from aorta/iliac arterial homogenates from 8 CON-V, 13 HF-V, 6 CON-M, and 8 HF-M mice. *$P < 0.05$ HF-V vs. all. V, vehicle; M, myriocin.

concentrations were normal in des1$^{+/-}$ mice (Supplementary Fig. 4*A–F*). Ceramide accumulation, endothelial dysfunction, and impaired eNOS phosphorylation were prevented in isolated aorta from des1$^{+/-}$ mice after palmitate incubation (Fig. 4*D–G*). Vascular smooth muscle responses were similar between groups (Fig. 4*F*). Thus, ceramide mediates palmitate-induced vascular dysfunction in vitro.

Ceramide biosynthesis impairs NO generation. To determine the mechanism by which de novo ceramide synthesis impairs the phosphorylation of eNOS and NO generation, BAECs were incubated with 500 µmol/L palmitate for 3 h. Palmitate exposure increased ceramide biosynthesis and decreased basal eNOS phosphorylation at Ser1177, eNOS dimer formation, and eNOS enzyme activity (Fig. 5*A–C* and *F–H*). All defects were reversed by myriocin. Agonist (i.e., insulin- and VEGF-) stimulated eNOS activation also was assessed. Insulin- and/or VEGF-stimulated eNOS phosphorylation at Ser1177 and Ser617 and NO generation were impaired by palmitate in a ceramide-dependent manner (Fig. 5*B–D* and *F*, *G*, and *I*). Specificity of our amperometric techniques was demonstrated by showing that insulin- and/or A23187-induced increases in NO_x production could be inhibited by N^G-monomethyl-L-arginine (not shown). Increased p-eNOS Thr495 or a reduced ratio of p-eNOS Ser1177 to Thr495 might render the eNOS enzyme refractory to agonist-induced stimuli (30). However, we observed no differences in p-eNOS Thr495 among treatments (Fig. 5*E*). No treatments promoted cell death when compared with vehicle treatment alone (not shown).

Ceramide biosynthesis does not disrupt Akt, AMPK, or ERK signaling to eNOS. Next we determined if ceramide-mediated inhibition of eNOS phosphorylation was secondary to defective upstream kinase signaling as previously suggested (14,31). In whole cell lysates from BAECs, palmitate did not impair insulin-stimulated phosphorylation of Akt at Ser473 or Thr308 or the Akt target, glycogen synthase kinase 3-β at Ser9 or ERK 1/2 phosphorylation (Fig. 6*A* and *B* and Supplementary Fig. 5*A*). Phosphorylation of AMPK (Thr172), or its target, acetyl Co-A carboxylase at Ser79 (Fig. 6*C* and Supplementary Fig. 5*B*), were not affected by any treatment. Thus palmitate-induced reductions in NO generation are not secondary to impaired upstream

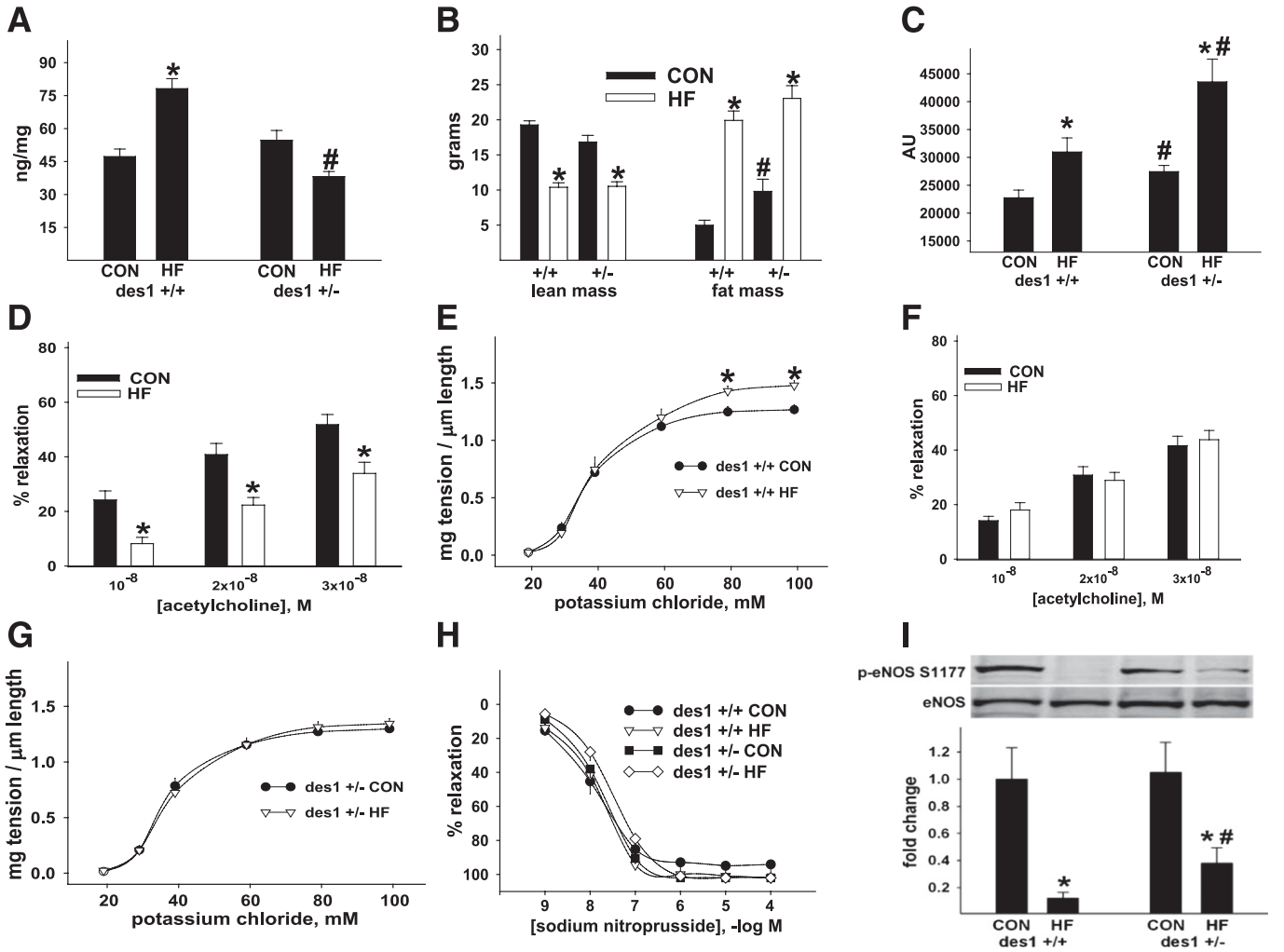

FIG. 3. Arterial function in fat-fed mice with targeted disruption of des1. des1$^{+/-}$ and des1$^{+/+}$ mice were placed on CON or HF diets for 3 months. Vascular ceramide content (*A*), body composition (*B*), and AUC during a glucose tolerance test (GTT) (*C*) in 9 HF des1$^{+/+}$, 11 HF des1$^{+/-}$, 12 CON des1$^{+/+}$, and 13 CON des1$^{+/-}$ mice. Fasting (6 h) blood glucose (mg/dL) before the GTT in panel *C* was higher in HF (164 ± 10) vs. CON des1$^{+/+}$ (122 ± 11) mice and HF (182 ± 11) vs. CON des1$^{+/-}$ (147 ± 9) animals. *D* and *E*: EDR and NR-mediated vasocontraction from HF vs. CON des1$^{+/+}$ mice. *F* and *G*: EDR and NR-mediated vasocontraction from HF vs. CON des1$^{+/-}$ mice. *H*: EIR from all groups. Data are from two femoral artery segments from each of the des1$^{+/+}$ and des1$^{+/-}$ mice. *I*: Representative immunoblot and densitometry of the ratio of p-eNOS Ser1177 to total eNOS from aorta/iliac arterial homogenates from des1$^{+/+}$ and des1$^{+/-}$ mice. *P < 0.05 CON vs. HF; #P < 0.05 des1$^{+/+}$ vs. des1$^{+/-}$. Results represent mean ± SEM. AU, arbitrary unit.

signaling to eNOS in endothelial cells under these experimental conditions.

Oxidative stress impairs basal but not insulin-stimulated eNOS phosphorylation in palmitate-treated BAECs. $O_2^{\cdot -}$ combining with NO to form peroxynitrite can disrupt eNOS dimer formation (32,33) and thereby reduce eNOS activity (33–35).We therefore evaluated if palmitate-induced $O_2^{\cdot -}$ production and peroxynitrite accumulation impaired basal or agonist-stimulated NO generation in a ceramide-dependent manner. Palmitate incubation (3 h × 500 μmol/L) increased ROS 3.2 ± 0.2 fold ($P < 0.05$, $n = 31$) as measured using dichlorofluorescein diacetate fluorescence. These findings were confirmed using ESR (Fig. 6*D*) and dihydroethidium staining (Supplementary Fig. 6). Further evidence of cellular oxidant stress was that palmitate exposure increased ($P < 0.05$) SOD-2 gene expression and SOD activity in a ceramide-dependent manner (not shown). Mitochondria appear to be the major source of palmitate-mediated ROS production by BAECs, and activation of NADPH-oxidase activity likely results from increased mitochondrial ROS production (Supplementary Fig. 7*A*–*F*).

Although 500 μmol/L palmitate evoked cellular oxidant stress, no evidence for peroxynitrite accumulation as estimated by nitrotyrosine enzyme-linked immunosorbent assay (Fig. 6*E*), Western blot, or immunohistochemistry (data not shown) could be detected. A 1.5-fold increase ($P <$ 0.05) in nitrotyrosine versus vehicle treatment was observed, however, when BAECs were incubated with 1,000 μmol/L palmitate for 3 h, a concentration that generated a greater increase in $O_2^{\cdot -}$ (i.e., 1.75-fold vs. vehicle treatment; $P <$ 0.05) in contrast to the 1.2-fold increase in cells exposed to 500 μmol/L palmitate (Fig. 6*D*). Therefore, high concentrations of palmitate (1,000 μmol/L) are sufficient to increase estimates of protein nitrosylation in a ceramide-dependent manner. However, ROS-mediated peroxynitrite accumulation is not the mechanism by which incubation of BAECs in 500 μmol/L palmitate leads to reductions of p-eNOS, eNOS dimer formation, or eNOS enzyme activity. No treatments increased cell death relative to vehicle alone (not shown).

Next we assessed the possibility that ceramide-evoked $O_2^{\cdot -}$ generation per se might mediate the suppression of basal and/or agonist-stimulated eNOS phosphorylation

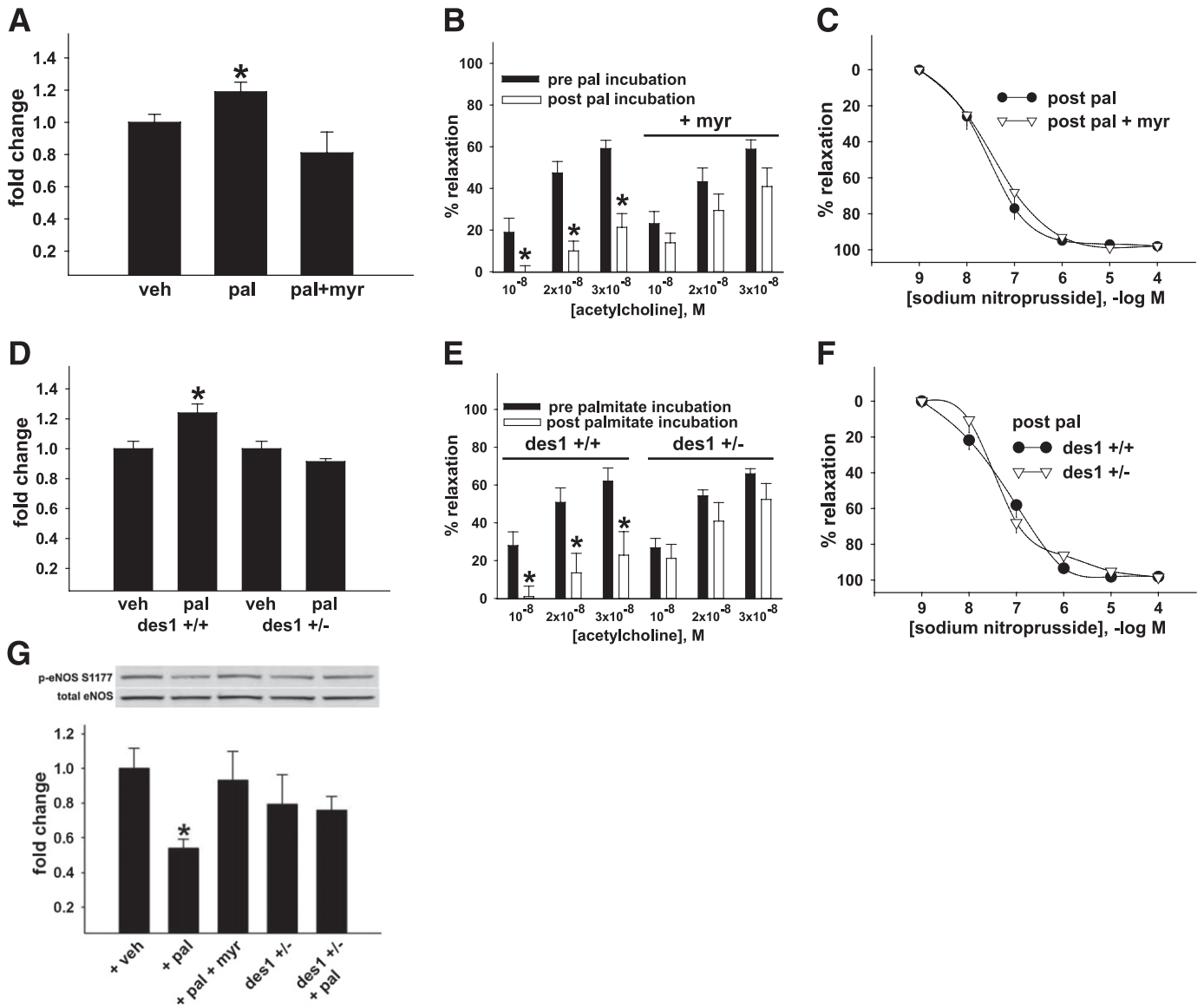

FIG. 4. Arterial function in isolated arteries from wild-type and des1$^{+/-}$ mice. Aorta from 10 C57Bl/6 mice were incubated with vehicle (veh), palmitate (pal), or pal + myriocin (myr). *A*: Pal-induced ceramide accumulation. *B*: EDR assessed in four femoral artery segments from the same 10 mice. Of these four segments, two were incubated with pal for 3 h while two were incubated with pal + myr for 3 h. *C*: EIR post pal ± myr treatment. *D*: Ceramide content in aorta from 6 des1$^{+/+}$ and des1$^{+/-}$ mice after treatment with veh or pal. *E*: EDR in vessels from des1$^{+/+}$ and des1$^{+/-}$ before and after 3-h pal treatment. *F*: EIR post pal in both genotypes. *G*: p-eNOS Ser1177 to total eNOS in aorta from wild-type mice (*lanes 1–3*) and in aorta from des1$^{+/-}$ mice (*lanes 4–5*) treated with or without pal (n = 5 segments per treatment). Representative blot (*upper*) and mean densitometry (*lower*). *P < 0.05 pre vs. post pal incubation. Results represent mean ± SEM.

(i.e., via a peroxynitrite-independent mechanism). BAECs were incubated with palmitate in the absence and presence of the intracellular $O_2^{\cdot -}$ scavenger dihydroxybenzene disulfonate (i.e., tiron). Palmitate-induced reductions of basal eNOS phosphorylation and eNOS dimer formation were negated when cells were treated with tiron. In contrast, insulin-induced p-eNOS Ser1177 and eNOS dimer formation were suppressed in palmitate-treated cells regardless of whether tiron was present (Fig. 6*F* and Supplementary Fig. 8*A* and *B*). However, when palmitate-treated cells were exposed to tiron plus myriocin, insulin-stimulated p-eNOS Ser1177 was fully restored (Fig. 6*F*). Collectively, under basal conditions, palmitate impairs eNOS enzyme function via mechanisms that are $O_2^{\cdot -}$ and ceramide dependent. Under insulin-stimulated conditions, palmitate impairs eNOS enzyme function via mechanisms that are $O_2^{\cdot -}$ independent and ceramide dependent.

Ceramide biosynthesis increases PP2A association with eNOS. We next examined the extent to which decreased agonist-stimulated eNOS activation in the presence of palmitate was secondary to increased dephosphorylation. We focused on PP2A, given earlier reports that ceramide increases PP2A activity (14,30,36). BAECs were incubated for 3 h in the absence and presence of palmitate, myriocin, and 4 nmol/L OA (the cell-permeable inhibitor of PP2A) (14,37). Vehicle or insulin was administered to BAECs for the last 10 min of each treatment period to assess basal and stimulated p-eNOS Ser1177 and NO production, respectively. We confirmed that palmitate-induced reductions in basal and insulin-stimulated p-eNOS Ser1177 and NO

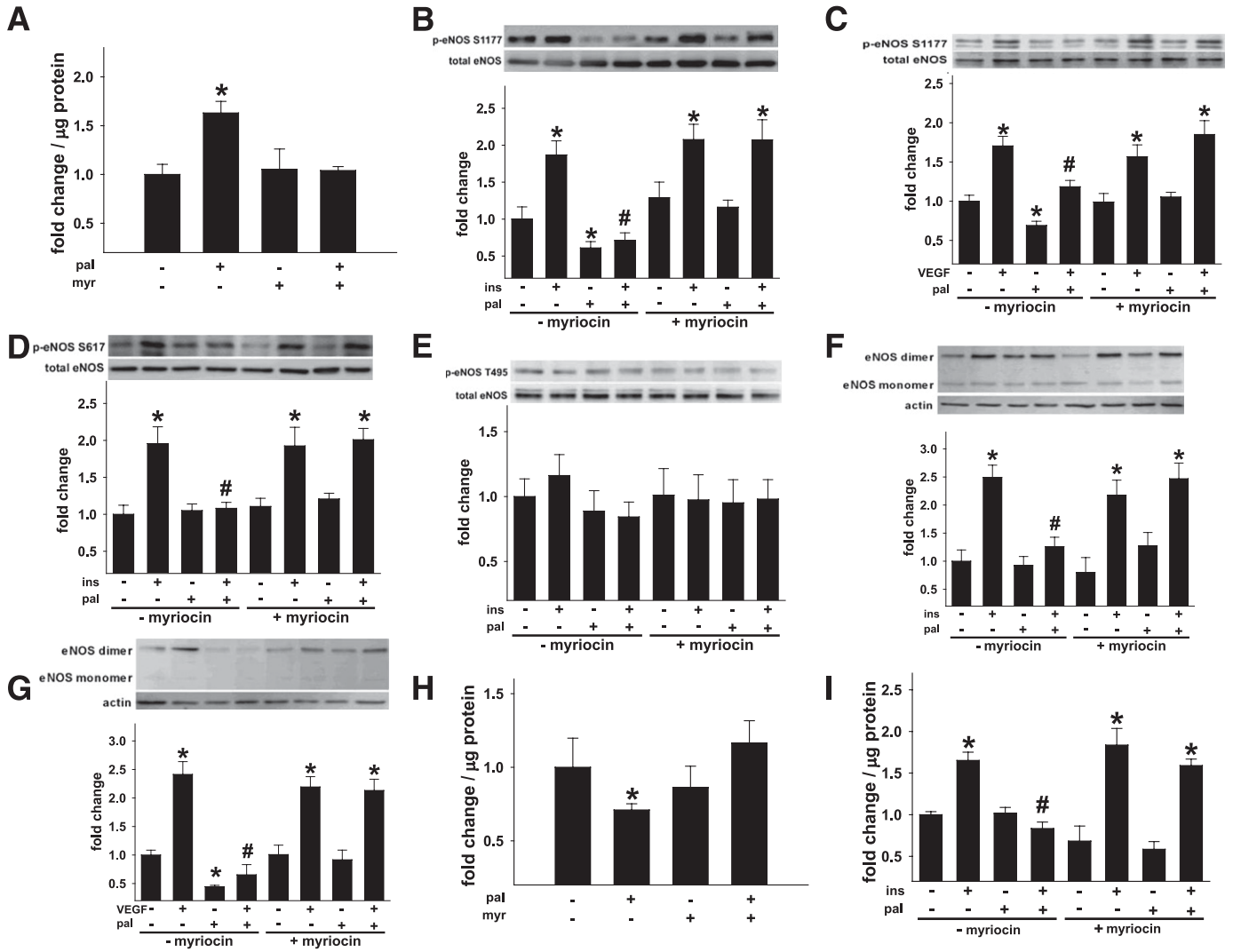

FIG. 5. Endogenous ceramide biosynthesis impairs NO generation. BAECs were incubated in the presence (+) or absence (−) of palmitate (pal) ± myriocin (myr). *A*: Pal-induced ceramide accrual (n = 6 per treatment). In some experiments, BAECs were treated for the last 10 min with vehicle (veh), insulin (ins), or VEGF. *B* and *C*: Basal (i.e., veh), ins-, or VEGF-stimulated p-eNOS Ser1177 to total eNOS (n = 10–32 per treatment). *D*: p-eNOS Ser617 (n = 15–19 per treatment). *E*: p-eNOS Thr495 to total eNOS (n = 10 per treatment). *F* and *G*: Ins- or VEGF-stimulated increases in the eNOS dimer to monomer ratio (n = 7–12 per treatment). *H*: NOS activity (n = 6–7 per treatment). *I*: Ins-mediated NO_x production (n = 10–15 per treatment). *P < 0.05 vs. respective veh treatment; #P < 0.05 vs. (+) ins or (+) VEGF and (−) pal. Results represent mean ± SEM.

production were prevented by myriocin. It is interesting that palmitate-induced reductions in basal and insulin-stimulated p-eNOS Ser1177 and NO production were prevented by OA (Fig. 7*A* and *B*).

To confirm a specific role for PP2A, expression levels of the catalytic subunit of PP2A in BAECs were reduced by ~70% using siRNA (Fig. 7*C*). BAECs expressing control (i.e., scrambled siRNA) and PP2A siRNA were treated with palmitate for 3 h before insulin stimulation for the last 10 min. Palmitate did not reduce basal or insulin-stimulated p-eNOS Ser1177 in PP2A deficient cells (Fig. 7*D*).

PP2A coimmunoprecipitated with eNOS in the presence of palmitate in a ceramide-dependent manner (Fig. 7*E* and Supplementary Fig. 9*A*). In cells treated identically, coimmunoprecipitation of Akt and Hsp90 with eNOS was negated by palmitate but restored by myriocin (Fig. 7*F* and *G* and Supplementary Fig. 9*B*). These relatively acute responses in cells were recapitulated in blood vessels from fat-fed des1$^{+/+}$ but not des1$^{+/-}$ mice. For example, PP2A coimmunoprecipitated with eNOS in arteries from fat-fed des1$^{+/+}$ but not des1$^{+/-}$ mice (Fig. 7*H*).

To test if the association of PP2A with eNOS prevents Akt from binding to eNOS, BAECs were incubated for 3 h in the absence and presence of palmitate and OA, after which cells were exposed to vehicle or insulin for the last 10 min. In the absence of OA, palmitate increased PP2A association with eNOS (Fig. 8*A*) and prevented Akt association with eNOS (Fig. 8*B*). In the presence of OA and palmitate, PP2A remained in the eNOS complex (Fig. 8*A*), but the insulin-stimulated association of Akt and eNOS was restored (Fig. 8*B*).

Next we determined whether PP2A might prevent phosphorylation of the pool of Akt that colocalizes with eNOS upon insulin stimulation. Palmitate prevented the phosphorylation by insulin of Akt at Ser473 and Thr308 and eNOS at Ser1177 in eNOS immunoprecipitates. This inhibition was reversed by OA (Fig. 8*C* and *D*).

The precise mechanism by which ceramide initiates PP2A colocalization with eNOS is unclear. We explored whether

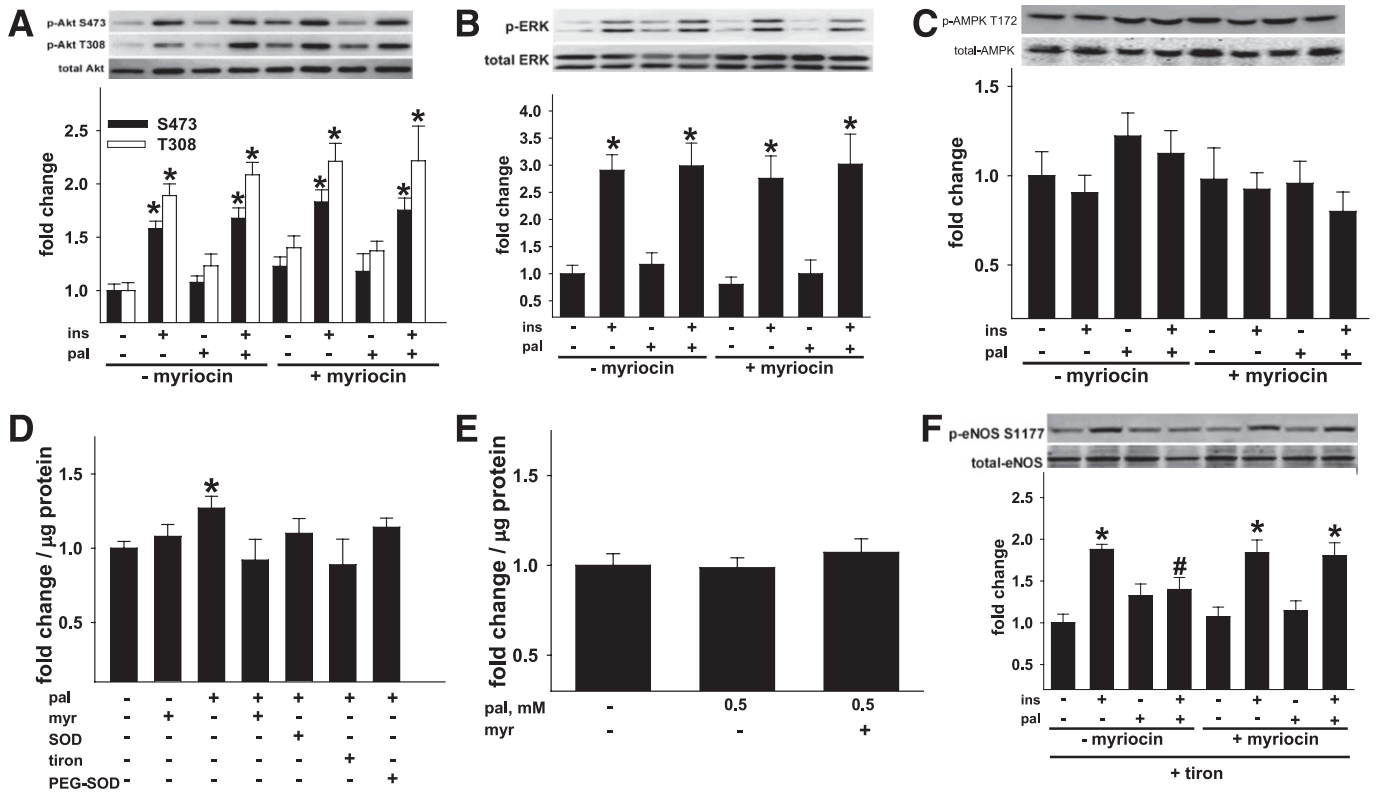

FIG. 6. Ceramide-associated changes in kinase signaling and $O_2^{\cdot -}$-mediated peroxynitrite formation. BAECs incubated ± pal ± myr for 3 h were treated for the last 10 min ± veh or ins. p-Akt Ser473 and Thr308 to total Akt (n = 12–37 per treatment) (*A*), p-AMPK T172 to total AMPK (n = 12–15 per treatment) (*B*), and p-ERK 1/2 to total ERK 1/2 (n = 13–27 per treatment) were not altered by pal (*C*). *D*: ESR indicated that 500 µmol/L pal increased cellular $O_2^{\cdot -}$ production and that responses could be negated by myr and the $O_2^{\cdot -}$ scavengers SOD, PEG-SOD, and tiron (n = 4–18 per treatment). *E*: Nitrotyrosine formation did not occur in response to 500 µmol/L pal (n = 8–16 per treatment). *F*: Pal-induced suppression of ins-stimulated p-eNOS to total eNOS could be restored by tiron + myr but not by tiron alone (n = 12–28 per treatment). *P < 0.05 vs. respective veh, #P < 0.05 vs. (+) ins (−) pal. Results represent mean ± SEM. Pal, palmitate; myr, myriocin; veh, vehicle; ins, insulin; PEG, polyethylene glycol.

palmitate-induced ceramide accumulation reduced the association between I2PP2A and PP2A. Immunoprecipitation experiments confirmed that palmitate reduced the association between I2PP2A and PP2A in a ceramide-dependent manner (Fig. 8*E* and Supplementary Fig. 9*C*).

Collectively, results from these experiments indicate that ceramide decreases the interaction between I2PP2A and PP2A, promoting PP2A association with eNOS. When this occurs, agonist-stimulated eNOS phosphorylation is attenuated either as a consequence of decreased phosphorylation of the pool of Akt that colocalizes with eNOS or by PP2A directly dephosphorylating eNOS. A synthesis of our findings is shown in Fig. 9.

DISCUSSION

We show for the first time that endogenous arterial ceramide accumulation in fat-fed mice precipitates endothelial dysfunction in a tissue-autonomous manner. These findings extend our previous study in which we reported that arterial dysfunction induced by fat feeding was independent of changes in insulin signaling in the vasculature (4). We now demonstrate that these changes can be recapitulated in isolated vessels and cultured cells by palmitate exposure and could be prevented by inhibiting the de novo synthesis of ceramide. In cultured endothelial cells, palmitate-induced, ceramide-mediated impairment in eNOS phosphorylation was independent of changes in activation of upstream kinases that phosphorylate eNOS or $O_2^{\cdot -}$-mediated peroxynitrite formation. We confirmed that palmitate and fat feeding activate PP2A to an extent that impairs eNOS phosphorylation in BAECs (14) and provide new insight into a novel mechanism by which ceramide-mediated PP2A activation prevents the phosphorylation of a pool of Akt that colocalizes with eNOS via Hsp90, thereby compromising full eNOS phosphorylation.

Prior studies of obese rodents reveal that ceramide inhibition could reverse glucose intolerance and delay the onset of diabetes (13,20–22). Blunting de novo ceramide synthesis could indirectly ameliorate endothelial dysfunction in obese mice by reducing the severity of circulating abnormalities associated with HF feeding, which have been shown to impair vascular function (reviewed in Creager et al., Imrie et al., Lüscher et al., and Williams et al.) (2,38–40). However, because exogenous synthetic ceramide impairs endothelium-dependent vasodilation and exaggerates vasoconstriction (reviewed in Li and in Alewijnse and Peters) (41,42), we reasoned that limiting endogenous ceramide biosynthesis might negate vascular dysfunction via direct mechanisms. Several studies evaluate the contribution from endogenous ceramide accumulation to cardiovascular complications associated with lipid oversupply. For example, Ser palmitoyl transferase 1 inhibition reduced the severity of aortic lesion formation in apolipoprotein E knockout mice that consumed an HF, high-cholesterol diet (23,24) and attenuated cardiac dysfunction and abnormal

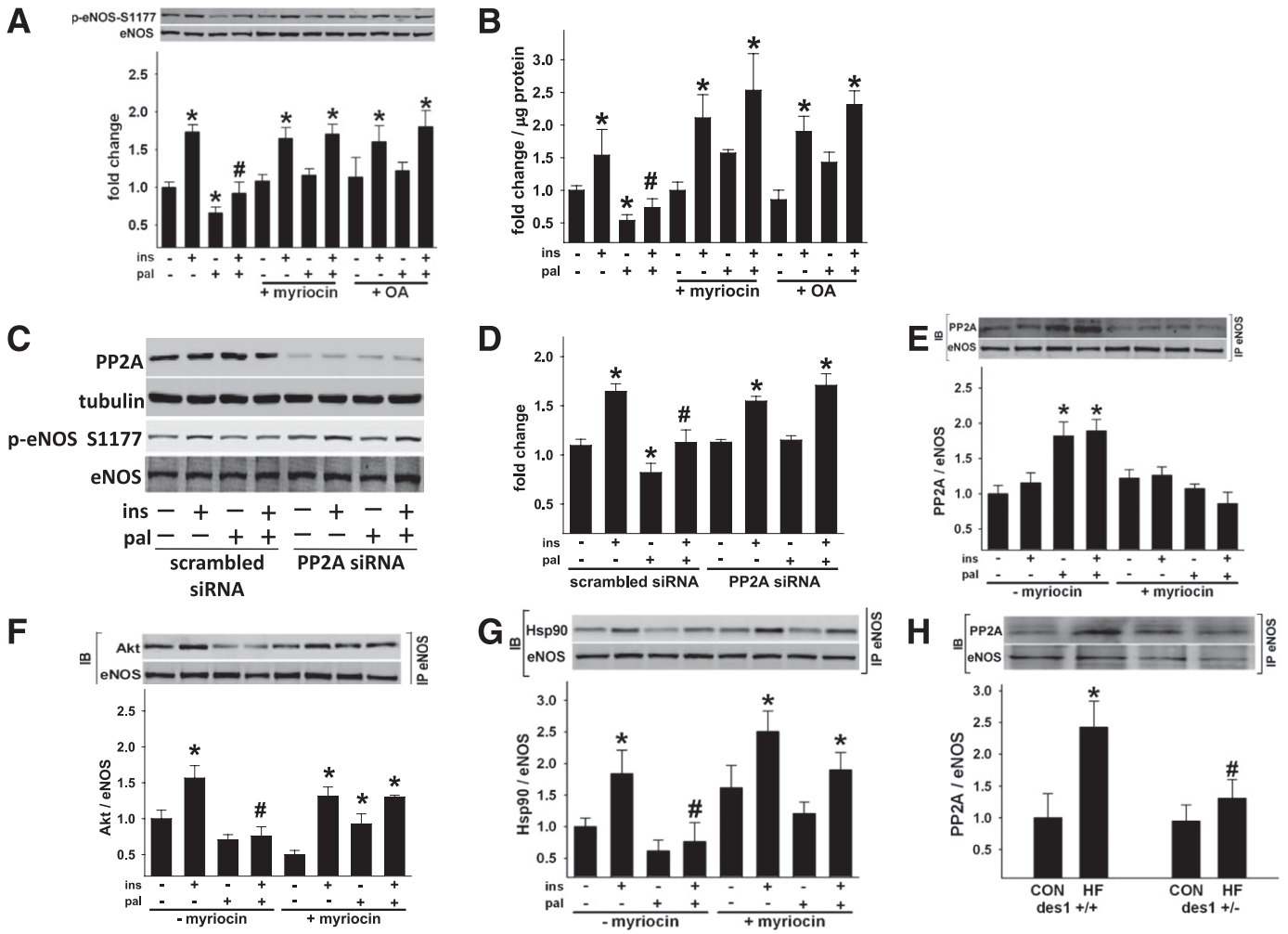

FIG. 7. Cellular ceramide biosynthesis impairs ins-stimulated p-eNOS in a PP2A-dependent manner. BAECs were incubated for 3 h ± pal ± myr or ± pal ± OA. For the last 10 min, BAECs were treated with veh or ins. p-eNOS(S)1177 (*A*) and NO_x production (*B*) in cells incubated with pal, myr, and OA as shown (*n* = 6–33 per treatment). *C*: Representative immunoblot showing impact of PP2A gene silencing on ins-mediated eNOS phosphorylation ± pal. *D*: The densitometry of six independent experiments are shown. *E–G*: BAECs were incubated ± pal ± myr. After eNOS immunoprecipitation (IP), a Western blot (IB) for PP2A, Akt, Hsp90, and eNOS was performed. *E*: Pal promotes PP2A association with eNOS in a ceramide-dependent manner (*n* = 9–11 per treatment). A reciprocal IP is shown in Supplementary Fig. 9*A*. *$P < 0.05$ vs. (−) ins (−) pal; #$P < 0.05$ vs. (+) ins (−) pal. *F* and *G*: A trend ($P = 0.05$) existed for pal to decrease Akt and Hsp90 association with eNOS. Pal prevented ins-stimulated Akt and Hsp90 association with eNOS in a ceramide-dependent manner (*n* = 5–8 per treatment). A reciprocal IP for Akt is shown in Supplementary Fig. 9*B*. *$P < 0.05$ vs. respective (−) ins, (−) pal treatment. *H*: In arterial homogenates from CON and HF des1$^{+/+}$ and des1$^{+/-}$ mice, an IP for eNOS was performed followed by an IB for PP2A (*n* = 5–6 per treatment). *$P < 0.05$ vs. CON, veh; #$P < 0.05$ vs. (+ ins) (− pal) (*F* and *G*) or vs. des1$^{+/+}$ (*H*). Results represent mean ± SEM. Pal, palmitate; myr, myriocin; veh, vehicle; ins, insulin.

substrate metabolism in hearts of mice with lipotoxic cardiomyopathy (43). It was recently reported that vascular ceramide accumulation, metabolic abnormalities, and endothelial dysfunction were limited in a rat model of severe hyperglycemia and obesity, after treatment with myriocin (13). Interpreting the results from that study is difficult because it is uncertain whether endothelial improvements were secondary to reduced vascular ceramide accrual or to improved systemic metabolism. We provide the first direct evidence that endothelial dysfunction, hypertension, and reduced arterial eNOS phosphorylation evoked by HF feeding are mediated to a significant degree by ceramide accumulation in the vasculature.

In endothelial cells, we showed that ceramide-induced inhibition of basal and agonist-stimulated eNOS phosphorylation and NO production was independent of altered signal transduction to eNOS and $O_2^{\cdot -}$-mediated peroxynitrite formation. A contribution from $O_2^{\cdot -}$ and ceramide was evident under basal conditions, however, as evidenced by the fact that palmitate-induced reduction in eNOS phosphorylation and dimer formation could be normalized by either tiron or myriocin. While the mechanism for $O_2^{\cdot -}$-related inhibition of eNOS phosphorylation under basal conditions remains to be clarified, we found no evidence for peroxynitrite formation using multiple independent assays under conditions in which eNOS phosphorylation and NO production were clearly impaired.

In light of these findings, and because eNOS phosphorylation is regulated by the balance of kinase and phosphatase activity (37), we evaluated if ceramide-induced activation of PP2A might be necessary and sufficient to prevent basal and insulin-stimulated eNOS phosphorylation (44,45). Myriocin and OA were equally effective in preventing palmitate-induced inhibition of insulin-stimulated eNOS phosphorylation at Ser617 and Ser1177. Furthermore, when PP2A was silenced in endothelial cells, palmitate failed to impair

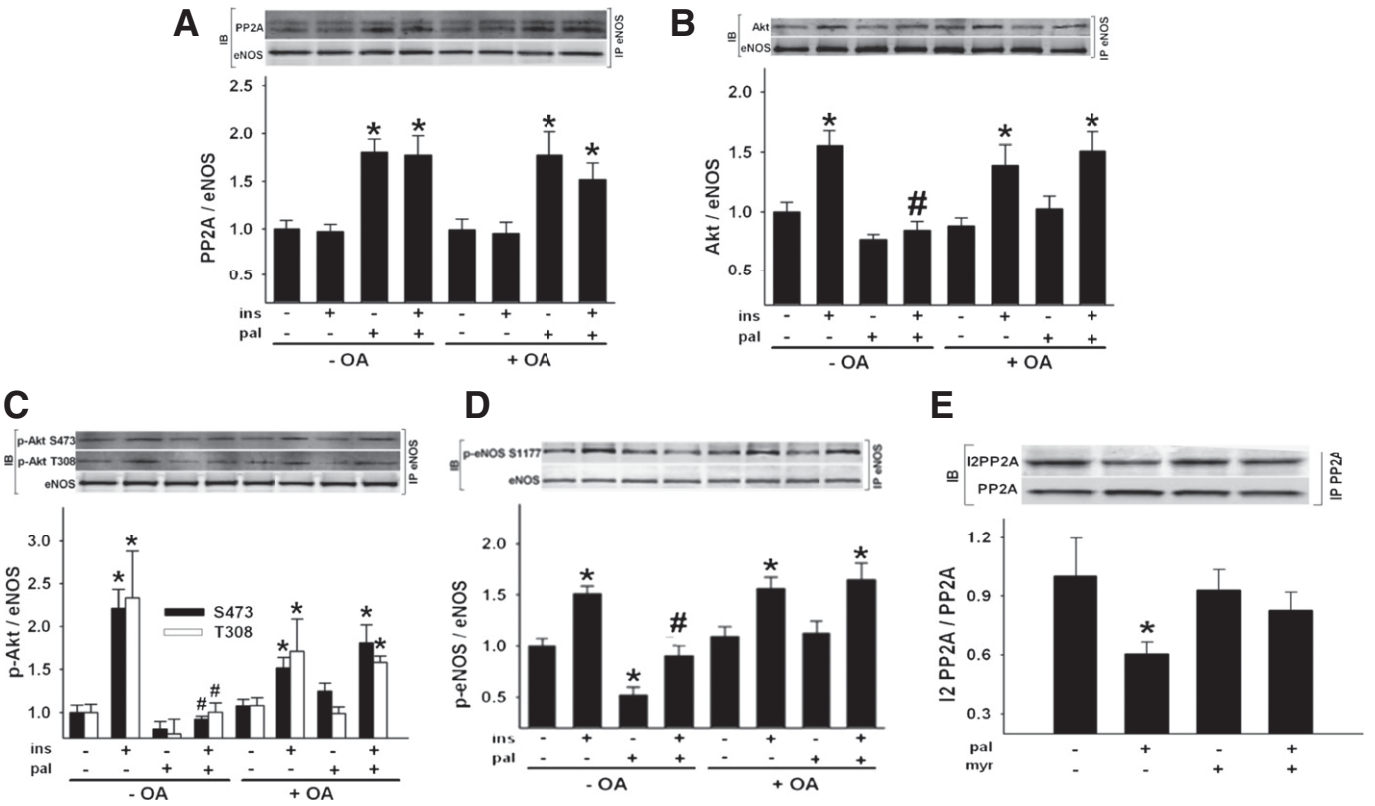

FIG. 8. PP2A promotes dephosphorylation of Akt that associates with eNOS. BAECs were incubated ± pal ± OA. For the last 10 min, cells were treated with veh or ins (*A–D*). After eNOS immunoprecipitation (IP), Western blot (IB) for PP2A, Akt, p-Akt, and eNOS was performed. *A*: PP2A association with eNOS (n = 12–34 per treatment). *B*: Akt association with eNOS (n = 13–35 per treatment). *C*: p-Akt Ser473 and p-Akt Thr308 association with eNOS (n = 6–8 per treatment). *D*: p-eNOS Ser1177 to total eNOS (n = 12–18 per treatment). *P < 0.05 vs. veh, #P < 0.05 vs. (−) pal (+) ins (−) OA. *E*: BAECs were incubated ± pal ± myr. After PP2A IP, IB for I2PP2A and PP2A was performed. I2PP2A that coimmunoprecipitated with PP2A was decreased by pal in a ceramide-dependent manner (n = 15–17 per treatment). A reciprocal IP is shown in Supplementary Fig. 9*C*. *P < 0.05 vs. (−) myr (−) pal; #P < 0.05 vs. (−) myr (+) pal. Results represent mean ± SEM. Pal, palmitate; myr, myriocin; veh, vehicle; ins, insulin.

insulin-stimulated eNOS phosphorylation. These data confirm an earlier investigation that PP2A is essential for palmitate-induced impairment in eNOS phosphorylation (14).

While results from previous studies suggest that eNOS phosphorylation might be attenuated secondary to ceramide-induced, PP2A-mediated dephosphorylation of Akt and/or AMPK (reviewed in Holland and Summers) (12), we observed no reduction in Akt, AMPK, or ERK phosphorylation in whole cell lysates in the presence of palmitate. We therefore explored if PP2A might reduce eNOS activation by impairing the subcellular pool of Akt that colocalizes with and phosphorylates eNOS. Earlier studies suggest that under certain conditions, primarily cytosolic PP2A can translocate to the membrane, associate directly with eNOS, and dephosphorylate eNOS at Ser1177 (46). Coimmunoprecipitation experiments confirmed that palmitate-induced association of PP2A with eNOS is ameliorated by myriocin, suggesting an essential role for ceramide in this interaction. While the compartmentalization and integration of signal transduction pathways at the cell membrane is complex, it currently is understood that Hsp90 might serve as a scaffold protein linking Akt to eNOS at caveolae (47,48). Indeed, we performed coimmunoprecipitation experiments and showed that basal and insulin-stimulated eNOS association with Hsp90 and Akt was inhibited by palmitate in a ceramide-dependent manner. These findings initially suggested that PP2A association with eNOS might impair Akt/Hsp90 binding to eNOS. However, we observed that palmitate-mediated inhibition of Akt and eNOS association was reversed by OA even though PP2A remained in the eNOS complex. We further observed that palmitate prevented insulin-stimulated Akt and eNOS phosphorylation in the eNOS immunoprecipitate in the absence but not the presence of OA. One interpretation of these data is that ceramide-mediated PP2A activation prevents the phosphorylation of a pool of Akt that colocalizes with eNOS. The data are also consistent with the possibility that PP2A dephosphorylates eNOS directly. Collectively, these ceramide-mediated molecular events limit full eNOS phosphorylation at Ser1177 and Ser617, impair NO bioavailability, and lead to vascular dysfunction.

The mechanisms by which ceramide promotes colocalization of PP2A with eNOS is incompletely understood. In addition to pharmacological inhibitors of PP2A (e.g., OA), noncompetitive biological inhibitors of PP2A exist. Inhibitor 1 of PP2A (I1PP2A) and I2PP2A associate with PP2A and inhibit its activity. It recently was shown in A549 human lung cancer cells that I2PP2A (but not I1PP2A) is a major ceramide-binding protein (49). Furthermore, the authors provided evidence that when ceramide binds to I2PP2A, the inhibition of I2PP2A on PP2A is relieved. We observed that palmitate-induced ceramide accumulation decreased the association between I2PP2A and PP2A, providing initial support for this potential mechanism of

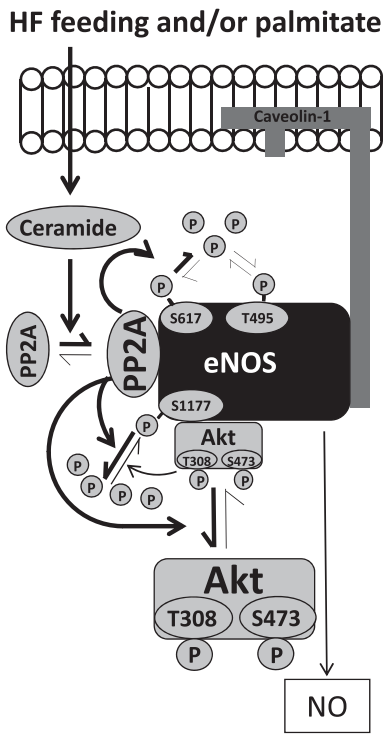

FIG. 9. Working model. HF feeding leads to arterial ceramide accumulation in vivo. Palmitate incubation elevates ceramide in isolated arteries and endothelial cells in vitro. Ceramide increases the association of PP2A with eNOS and decreases the association between eNOS and Akt and between eNOS and Hsp90. PP2A promotes the dephosphorylation of Akt that colocalizes with eNOS and/or decreases eNOS phosphorylation at Ser1177 and Ser617 directly. This impairs NO bioavailability and leads to vascular dysfunction.

action in the context of our experimental conditions. Collectively, these results suggest that by disrupting the association with I2PP2A, ceramide will promote the association of PP2A with eNOS. The presence of PP2A in the Akt/Hsp90/eNOS complex impairs Akt phosphorylation (likely by direct dephosphorylation) and decreases eNOS phosphorylation by a similar mechanism, or indirectly as a consequence of reduced Akt activation.

Ceramide regulates diverse cellular processes via mechanisms that are not completely understood, and its role in the pathogenesis of cardiovascular disease has not been fully elucidated (reviewed in Holland and Summers, Chavez and Summers, and Summers and Nelson) (12,15,50). We determined its contribution to vascular dysfunction associated with lipid overload (41,42). Our results are the first to show that de novo ceramide biosynthesis contributes directly to vascular dysfunction and hypertension that characterizes diet-induced obesity. Findings from isolated vessels and endothelial cells indicate that ceramide impairs the association of p-Akt with eNOS in a PP2A-dependent manner, leading to reduced eNOS activation and endothelial dysfunction. These data provide mechanistic insights linking endogenous vascular ceramide biosynthesis to cardiovascular defects in a murine model of diet-induced obesity and type 2 diabetes and present new targets for the treatment of vascular dysfunction in these prevalent conditions.

ACKNOWLEDGMENTS

This work was funded, in part, by the University of Utah College of Health, the University of Utah Research Foundation, American Heart Association (AHA) Western States Affiliate Grant-In-Aid 06-55222Y, American Diabetes Association Research Grant 7-08-RA-164, and National Institutes of Health grants R15-HL-091493-01 (to J.D.S.), F32-DK-083866 (to W.L.H.), and RO1-HL-070070 to E.D.A. E.D.A. is an established investigator of the AHA. Student support was provided, in part, by the AHA Western States Affiliate Summer Student Research Program, the American Physiological Society Undergraduate Research Fellowship Program, the University of Utah Undergraduate Research Opportunities Program, and Short-Term Training: Students in Health Professional Schools Grant T35-HL-007744.

No potential conflicts of interest relevant to this article were reported.

Q.-J.Z. researched data, assisted with experimental design, and wrote the manuscript. W.L.H. researched data, assisted with experimental design, and wrote, reviewed, and edited the manuscript. L.W., J.M.T., J.M.C., D.P., D.G., T.R., and J.R. (cell culture experiments); D.K., J.L., B.D., and C.A.K. (vascular reactivity experiments); and N.D., A.N., and M.D. (metabolism experiments) researched data as University of Utah undergraduate students. C.A. researched data as a 2nd year University of Utah medical student. C.B. and D.R.M. facilitated the ESR measurements. K.A. and K.K.N. researched data as University of Utah graduate students. S.A.S. and E.D.A. reviewed and edited the manuscript. J.D.S. researched data and wrote, reviewed, and edited the manuscript. J.D.S. is the guarantor of this work and, as such, had full access to all of the data in the study and takes responsibility for the integrity of the data and the accuracy of the data analysis.

Parts of this study were presented in abstract form at Experimental Biology 2008, San Diego, California, 5–9 April 2008; Experimental Biology 2010, Anaheim, California, 24–28 April 2010; Experimental Biology 2011, Washington, DC, 9–13 April 2011; and at the 69th and 71st Scientific Sessions of the American Diabetes Association, New Orleans, Louisiana, 5–9 June 2009, and San Diego, California, 24–28 June 2011, respectively.

REFERENCES

1. Centers for Disease Control and Prevention. National diabetes fact sheet: general information and national estimates on diabetes in the United States, 2007 [article online], 2008. Atlanta, GA, U.S. Department of Health and Human Services. Available from http://www.cdc.gov/diabetes/pubs/pdf/ndfs_2007.pdf. Accessed August 2011
2. Creager MA, Lüscher TF, Cosentino F, Beckman JA. Diabetes and vascular disease: pathophysiology, clinical consequences, and medical therapy: Part I. Circulation 2003;108:1527–1532
3. Kim F, Tysseling KA, Rice J, et al. Free fatty acid impairment of nitric oxide production in endothelial cells is mediated by IKKbeta. Arterioscler Thromb Vasc Biol 2005;25:989–994
4. Symons JD, McMillin SL, Riehle C, et al. Contribution of insulin and Akt1 signaling to endothelial nitric oxide synthase in the regulation of endothelial function and blood pressure. Circ Res 2009;104:1085–1094
5. Edirisinghe I, McCormick Hallam K, Kappagoda CT. Effect of fatty acids on endothelium-dependent relaxation in the rabbit aorta. Clin Sci (Lond) 2006;111:145–151
6. Du X, Edelstein D, Obici S, Higham N, Zou MH, Brownlee M. Insulin resistance reduces arterial prostacyclin synthase and eNOS activities by increasing endothelial fatty acid oxidation. J Clin Invest 2006;116:1071–1080
7. Steinberg HO, Paradisi G, Hook G, Crowder K, Cronin J, Baron AD. Free fatty acid elevation impairs insulin-mediated vasodilation and nitric oxide production. Diabetes 2000;49:1231–1238
8. Alderton WK, Cooper CE, Knowles RG. Nitric oxide synthases: structure, function and inhibition. Biochem J 2001;357:593–615
9. Shaul PW. Regulation of endothelial nitric oxide synthase: location, location, location. Annu Rev Physiol 2002;64:749–774
10. Sessa WC. eNOS at a glance. J Cell Sci 2004;117:2427–2429
11. Summers SA. Sphingolipids and insulin resistance: the five Ws. Curr Opin Lipidol 2010;21:128–135

12. Holland WL, Summers SA. Sphingolipids, insulin resistance, and metabolic disease: new insights from in vivo manipulation of sphingolipid metabolism. Endocr Rev 2008;29:381–402
13. Chun L, Junlin Z, Aimin W, Niansheng L, Benmei C, Minxiang L. Inhibition of ceramide synthesis reverses endothelial dysfunction and atherosclerosis in streptozotocin-induced diabetic rats. Diabetes Res Clin Pract 2011;93:77–85
14. Wu Y, Song P, Xu J, Zhang M, Zou MH. Activation of protein phosphatase 2A by palmitate inhibits AMP-activated protein kinase. J Biol Chem 2007; 282:9777–9788
15. Chavez JA, Summers SA. Lipid oversupply, selective insulin resistance, and lipotoxicity: molecular mechanisms. Biochim Biophys Acta 2010;1801: 252–265
16. Zhang DX, Zou AP, Li PL. Ceramide-induced activation of NADPH oxidase and endothelial dysfunction in small coronary arteries. Am J Physiol Heart Circ Physiol 2003;284:H605–H612
17. Zheng T, Li W, Wang J, Altura BT, Altura BM. Sphingomyelinase and ceramide analogs induce contraction and rises in [Ca(2+)](i) in canine cerebral vascular muscle. Am J Physiol Heart Circ Physiol 2000;278:H1421–H1428
18. Li H, Junk P, Huwiler A, et al. Dual effect of ceramide on human endothelial cells: induction of oxidative stress and transcriptional upregulation of endothelial nitric oxide synthase. Circulation 2002;106:2250–2256
19. Holland WL, Brozinick JT, Wang L-P, et al. Inhibition of ceramide synthesis ameliorates glucocorticoid-, saturated-fat-, and obesity-induced insulin resistance. Cell Metab 2007;5:167–179
20. Ussher JR, Koves TR, Cadete VJ, et al. Inhibition of de novo ceramide synthesis reverses diet-induced insulin resistance and enhances whole-body oxygen consumption. Diabetes 2010;59:2453–2464
21. Shah C, Yang G, Lee I, Bielawski J, Hannun YA, Samad F. Protection from high fat diet-induced increase in ceramide in mice lacking plasminogen activator inhibitor 1. J Biol Chem 2008;283:13538–13548
22. Yang G, Badeanlou L, Bielawski J, Roberts AJ, Hannun YA, Samad F. Central role of ceramide biosynthesis in body weight regulation, energy metabolism, and the metabolic syndrome. Am J Physiol Endocrinol Metab 2009;297:E211–E224
23. Park TS, Panek RL, Mueller SB, et al. Inhibition of sphingomyelin synthesis reduces atherogenesis in apolipoprotein E-knockout mice. Circulation 2004;110:3465–3471
24. Hojjati MR, Li Z, Zhou H, et al. Effect of myriocin on plasma sphingolipid metabolism and atherosclerosis in apoE-deficient mice. J Biol Chem 2005; 280:10284–10289
25. Zhang QJ, McMillin SL, Tanner JM, Palionyte M, Abel ED, Symons JD. Endothelial nitric oxide synthase phosphorylation in treadmill-running mice: role of vascular signalling kinases. J Physiol 2009;587:3911–3920
26. Symons JD, Hu P, Yang Y, et al. Knockout of insulin receptors in cardiomyocytes attenuates coronary arterial dysfunction induced by pressure overload. Am J Physiol Heart Circ Physiol 2011;300:H374–H381
27. Perry DK, Bielawska A, Hannun YA. Quantitative determination of ceramide using diglyceride kinase. Methods Enzymol 2000;312:22–31
28. Sullards MC, Merrill AH Jr. Analysis of sphingosine 1-phosphate, ceramides, and other bioactive sphingolipids by high-performance liquid chromatography-tandem mass spectrometry. Sci STKE 2001;2001:pl1
29. Reaven GM, Hollenbeck C, Jeng CY, Wu MS, Chen YD. Measurement of plasma glucose, free fatty acid, lactate, and insulin for 24 h in patients with NIDDM. Diabetes 1988;37:1020–1024
30. Smith AR, Visioli F, Frei B, Hagen TM. Age-related changes in endothelial nitric oxide synthase phosphorylation and nitric oxide dependent vasodilation: evidence for a novel mechanism involving sphingomyelinase and ceramide-activated phosphatase 2A. Aging Cell 2006;5:391–400
31. Rodríguez-Crespo I, Moënne-Loccoz P, Loehr TM, Ortiz de Montellano PR. Endothelial nitric oxide synthase: modulations of the distal heme site produced by progressive N-terminal deletions. Biochemistry 1997;36:8530–8538
32. Chavez JA, Summers SA. Characterizing the effects of saturated fatty acids on insulin signaling and ceramide and diacylglycerol accumulation in 3T3-L1 adipocytes and C2C12 myotubes. Arch Biochem Biophys 2003;419:101–109
33. Molnar J, Yu S, Mzhavia N, Pau C, Chereshnev I, Dansky HM. Diabetes induces endothelial dysfunction but does not increase neointimal formation in high-fat diet fed C57BL/6J mice. Circ Res 2005;96:1178–1184
34. Zou MH, Shi C, Cohen RA. Oxidation of the zinc-thiolate complex and uncoupling of endothelial nitric oxide synthase by peroxynitrite. J Clin Invest 2002;109:817–826
35. Fonseca FV, Ravi K, Wiseman D, et al. Mass spectroscopy and molecular modeling predict endothelial nitric oxide synthase dimer collapse by hydrogen peroxide through zinc tetrathiolate metal-binding site disruption. DNA Cell Biol 2010;29:149–160
36. Chavez JA, Knotts TA, Wang L-P, et al. A role for ceramide, but not diacylglycerol, in the antagonism of insulin signal transduction by saturated fatty acids. J Biol Chem 2003;278:10297–10303
37. Millward TA, Zolnierowicz S, Hemmings BA. Regulation of protein kinase cascades by protein phosphatase 2A. Trends Biochem Sci 1999;24:186–191
38. Imrie H, Abbas A, Kearney M. Insulin resistance, lipotoxicity and endothelial dysfunction. Biochim Biophys Acta 2010;1801:320–326
39. Lüscher TF, Creager MA, Beckman JA, Cosentino F. Diabetes and vascular disease: pathophysiology, clinical consequences, and medical therapy: Part II. Circulation 2003;108:1655–1661
40. Williams IL, Wheatcroft SB, Shah AM, Kearney MT. Obesity, atherosclerosis and the vascular endothelium: mechanisms of reduced nitric oxide bioavailability in obese humans. Int J Obes Relat Metab Disord 2002;26: 754–764
41. Li X, Becker KA, Zhang Y. Ceramide in redox signaling and cardiovascular diseases. Cell Physiol Biochem 2010;26:41–48
42. Alewijnse AE, Peters SL. Sphingolipid signalling in the cardiovascular system: good, bad or both? Eur J Pharmacol 2008;585:292–302
43. Park TS, Hu Y, Noh HL, et al. Ceramide is a cardiotoxin in lipotoxic cardiomyopathy. J Lipid Res 2008;49:2101–2112
44. Michell BJ, Chen Zp, Tiganis T, et al. Coordinated control of endothelial nitric-oxide synthase phosphorylation by protein kinase C and the cAMP-dependent protein kinase. J Biol Chem 2001;276:17625–17628
45. Greif DM, Kou R, Michel T. Site-specific dephosphorylation of endothelial nitric oxide synthase by protein phosphatase 2A: evidence for crosstalk between phosphorylation sites. Biochemistry 2002;41:15845–15853
46. Wei Q, Xia Y. Proteasome inhibition down-regulates endothelial nitric-oxide synthase phosphorylation and function. J Biol Chem 2006;281:21652–21659
47. Shiojima I, Walsh K. Role of Akt signaling in vascular homeostasis and angiogenesis. Circ Res 2002;90:1243–1250
48. Fontana J, Fulton D, Chen Y, et al. Domain mapping studies reveal that the M domain of hsp90 serves as a molecular scaffold to regulate Akt-dependent phosphorylation of endothelial nitric oxide synthase and NO release. Circ Res 2002;90:866–873
49. Mukhopadhyay A, Saddoughi SA, Song P, et al. Direct interaction between the inhibitor 2 and ceramide via sphingolipid-protein binding is involved in the regulation of protein phosphatase 2A activity and signaling. FASEB J 2009;23:751–763
50. Summers SA, Nelson DH. A role for sphingolipids in producing the common features of type 2 diabetes, metabolic syndrome X, and Cushing's syndrome. Diabetes 2005;54:591–602